J. Fluid Mech. (2002), *vol.* 471, *pp.* 33–50.
DOI: 10.1017/S0022112002002082 Printed in the United Kingdom

The mixing in a room by a localized finite-mass-flux source of buoyancy

By C. P. CAULFIELD[1] AND ANDREW W. WOODS[2]

[1]Department of Mechanical and Aerospace Engineering, University of California, San Diego, 9500 Gilman Drive, La Jolla, CA 92093-0411, USA

[2]BP Institute for Multiphase Flows, University of Cambridge, Madingley Road, Cambridge CB3 OEZ, UK

(Received 23 November 2001 and in revised form 14 February 2002)

The mixing produced by a turbulent buoyant plume with finite mass flux in a room is examined analytically and numerically. The entrainment of ambient fluid into the ascending buoyant plume leads to a return flow in the room which carries fluid downwards from the top of the room. The cycling of ambient fluid through the buoyant plume and the return flow causes the density to become uniform and gradually evolve towards that of the source fluid. As a result the buoyancy flux associated with the input fluid decreases and the plume motion becomes dominated by the source momentum flux. We develop an asymptotic model of the mixing using buoyant plume theory for a momentum-dominated flow. This provides an analytical description of the evolution of the density in the room which is in excellent accord with a full numerical simulation, and provides an improved description of the experimental filling-box data originally presented by Baines & Turner (1969).

1. Introduction

In a number of industrial processes, highly volatile fluids are stored under pressure in the liquid phase. Important examples include liquid chlorine, which is used for purification purposes in the water industry, and liquid natural gas (LNG). If the pipework associated with the storage tanks of these liquids fails, the liquid escapes from the tank and on decompression vaporizes and cools, typically producing a source of dense hazardous gas. When such a rupture occurs within a building, the gas may contaminate the building before ultimately venting into the atmosphere. Knowledge of the mixing processes within the building is key for predicting the concentration of the contaminated air which may vent from the building, as well as for the positioning of gas detectors and the design of evacuation strategies from the contaminated building. Similar mixing processes may arise with some air-conditioning systems in which cold air is supplied to a room from a heat exchanger which removes warm air from the room. This process drives buoyant convection, which cools the room and thereby alters the density distribution within the room. Again, knowledge of the mixing process induced by the injection of the cool air is important for positioning of thermostats regulating the air-conditioners, as well as for the design of energy-efficient cooling systems.

Motivated by such problems, there has been substantial interest in the mixing within a confined room produced by a buoyant plume, originating from a source of buoyancy. This has built upon the classical work of Morton, Taylor & Turner (1956),

in which a quantitative model for the motion of a Boussinesq turbulent buoyant plume was first developed and tested with laboratory experiments. That model considers the vertical variation of the horizontally averaged and time-averaged volume flux, πQ, specific momentum flux, πM, and specific buoyancy flux πF, defined as

$$Q(z) = 2\int_0^\infty w_p r \,\mathrm{d}r = \overline{w_p} b^2, \tag{1.1}$$

$$M(z) = 2\int_0^\infty w_p^2 r \,\mathrm{d}r = \overline{w_p}^2 b^2, \tag{1.2}$$

$$F(z) = 2\int_0^\infty g\frac{(\rho_a - \rho_p)}{\rho_0} w_p r \,\mathrm{d}r = g\frac{\rho_a - \overline{\rho_p}}{\rho_0}\overline{w_p} b^2 \equiv g'Q, \tag{1.3}$$

where $w_p(r,z)$ and $\rho_p(r,z)$ are the axisymmetric, time-averaged vertical velocity and density distribution within the plume, ρ_a is the ambient density, ρ_0 is a reference density, g' is the reduced gravity, and we have defined, for simplicity, the equivalent top-hat values of the plume density $\overline{\rho}_p(z)$ and vertical velocity $\overline{w}_p(z)$, which are constant within the plume, of characteristic radius $b(z)$, and zero outside. Density variations from the reference density are assumed to be sufficiently small so that their only significant effect is on the buoyancy within the flow. These averaged fluxes satisfy

$$\frac{\mathrm{d}Q}{\mathrm{d}z} = 2\epsilon M^{1/2}, \tag{1.4}$$

$$M\frac{\mathrm{d}M}{\mathrm{d}z} = FQ, \tag{1.5}$$

$$\frac{\mathrm{d}F}{\mathrm{d}z} = \frac{g}{\rho_0}\frac{\mathrm{d}\rho_a}{\mathrm{d}z}Q, \tag{1.6}$$

where ϵ is an empirically determined entrainment coefficient (see Morton *et al.* 1956; Turner 1979, 1986 for more discussion) appropriate for top-hat models. The entrainment constant ϵ takes different values for momentum-driven jets and buoyant plumes (Turner 1986). In the present work, we find that as the flow slowly evolves over time scales for which the source mass flux is important, then after an initial transient, the plume dynamics are little affected by the source buoyancy flux and we expect that the entrainment process may be accurately modelled using a value of ϵ appropriate for jet-like flows. As discussed in §4 when we apply our predictions to the previously reported experiments of Baines & Turner (1969, hereinafter referred to as BT69) within an experiment it is possible to infer the actual effective value of the entrainment constant directly for the particular source and flow geometry.

BT69 demonstrated that in a confined room, of sufficiently small aspect ratio, the entrainment of ambient fluid by the plume leads to a return flow in the room. If the cross-sectional area of the room is sufficiently large so that at all heights within the room the plume occupies a negligible fraction of the cross-sectional area of the room A, then the return flow is nearly uniform and given by the volume conservation relation

$$wA = -\pi Q. \tag{1.7}$$

In the limit, $b^2 \ll A$, the ambient density within the room $\rho_a(z,t)$ evolves on a much longer time scale than that of the buoyant plume. Thus, assuming that the diffusive transport is negligible on the relatively short time scale of the convective flow, the

equation for the downward advection of density surfaces ρ_a, is

$$\frac{\partial \rho_a}{\partial t} + w\frac{\partial \rho_a}{\partial z} = 0. \tag{1.8}$$

These relations describe the filling-box process associated with a turbulent buoyant plume in a confined room. BT69 solved these equations asymptotically to describe the late-time density evolution of the ambient fluid, as the continuing plume supplies fluid to the top of the room, under the assumptions that eventually: the region contaminated by plume fluid occupies virtually the whole depth of the room; the buoyancy from the plume is uniformly distributed throughout the room through the process of entrainment; and the density within the room varies at a constant rate with time. This model was used to describe laboratory experiments of the filling-box process, with some deviation, as discussed in more detail in § 4.

Germeles (1975) introduced a more sophisticated numerical scheme to examine the effect of a source of mass and momentum in addition to the buoyancy. This did not introduce any substantial differences in the plume behaviour over the filling-box time scale. In a related study, Worster & Huppert (1983, hereinafter referred to as WH83) developed the model presented by BT69 further by accounting for the actual time-dependent variation of the depth of the contaminated region in the evolution of the asymptotic solution for the density distribution in the room, while still assuming that the buoyancy of the plume is distributed uniformly in space within the contaminated region. This model was shown to agree well with full numerical solutions of plume equations, when the source conditions were defined as a pure source of buoyancy. However, there is a singularity in the buoyancy at the source if the source buoyancy flux is finite while the source volume flux is zero. Therefore, there is no well-defined extremal density within the flow, and in principle the mean density within the room can decrease without limit. Also, since there is zero volume flux from the source, the return flow never reaches the actual level of the source, and the model predicts a zone of sharp stratification in the ambient fluid just above the source.

In many real problems, the source of buoyancy may also involve a source of mass. As a result, the source density difference remains finite, and this leads to important differences in the predictions of the model at long times compared to idealized models which neglect the mass flux. The purpose of this paper is to examine the long-term mixing driven by the source of buoyant fluid, accounting for the mass flux and associated ventilation flow from the room. Now there is a well-defined minimum density (the source fluid density) for the fluid within the room, and so the room density must eventually approach the density of the input fluid. We focus on the evolution of the density profile in the room and the density of the fluid which vents from the room into the neighbouring environment.

In § 2 we describe the model and develop some asymptotic solutions for the case in which the plume momentum flux does not evolve significantly over the depth of the room, assuming that the ventilation opening is at the same level as the source. We compare this with numerical solutions of the plume equations in § 3, including cases in which the source fluid initially has significant buoyancy flux, and so the momentum flux of the plume evolves significantly over the depth of the layer, at least during an initial transient. We compare our theoretical model with the experimental results of BT69 in § 4, and then present a specific application of our work in § 5. Finally, we draw some conclusions in § 6.

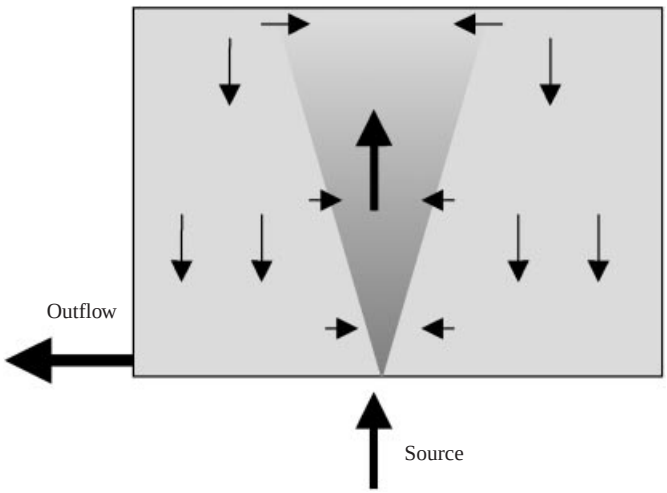

FIGURE 1. Schematic of the flow through a ventilated room with an isolated source of mass and buoyancy and a single opening at the height of the source.

2. The long-time limit of the ventilated filling box

We adopt the model of the turbulent buoyant plume (1.4)–(1.6) introduced by Morton *et al.* (1956), and combine this with the model for return flow (1.8). We assume that the ambient fluid within the room initially has uniform density, $\rho_a(z,0) = \rho_{a0}$. We also assume there is a plume at the base of the room $z = 0$ with source volume flux πQ_s and density ρ_s, which is smaller than the initial value of the ambient density at the floor of the room, $\rho_a(0,0) = \rho_{a0}$. In addition, for simplicity, we assume that the vent is exactly at the same height as the source $z = 0$, that the vent is of zero depth, and that the flow through it is purely outwards. We assume that the filling-box flow develops as described in BT69. In order that the boundary walls do not interfere with the flow, we require that the aspect ratio (i.e. the height H divided by the square root of the cross-sectional area A) of the room is sufficiently small (see BT69; Hunt, Cooper & Linden 2001). This situation is shown schematically in figure 1. Once the source flux begins to flow, an equal flux, πQ_s, will start to vent through the opening. Initially, the density of the fluid which vents is $\rho_v = \rho_{a0}$. However, since the volume flux in the plume is finite, the return flow is also finite. Therefore, after a finite time, the first front descends to the elevation of the opening and contaminated fluid starts to be vented. The subsequent outflow becomes progressively more contaminated by source fluid, and, as time increases, $\rho_a(0,t) = \rho_v(t) \to \rho_s$.

Once the return flow transports plume fluid through the ambient and back to the same elevation as the source $z = 0$, the reduced gravity g'_s and the effective buoyancy flux F_s of the source decrease from their initial values of g'_0 and F_0, i.e.

$$F_s = \frac{g(\rho_a(0,t) - \rho_s)Q_s}{\rho_0} = g'_s Q_s \leqslant F_0 = \frac{g(\rho_{a0} - \rho_s)Q_s}{\rho_0} = g'_0 Q_s. \tag{2.1}$$

Equation (1.5) illustrates that in a room of height H, the change in momentum flux of a buoyant plume with source specific momentum flux πM_s, volume flux πQ_s and buoyancy flux πF_s, is negligible if

$$P(t) = \frac{5F_s Q_s H}{4M_s^2} \ll 1, \quad P(t) \leqslant P(0) \equiv P_0. \tag{2.2}$$

If the condition that $P(t) \ll 1$ in (2.2) is satisfied for all time, then the mass flux in the plume varies with height above the source, $z = 0$, according to the approximate relation (see (1.4))

$$Q(\zeta) = Q_s(1 + \theta\zeta), \tag{2.3}$$

where

$$\theta = \frac{2\epsilon M_s^{1/2} H}{Q_s}, \quad \zeta = \frac{z}{H}. \tag{2.4}$$

The quantity θ represents a non-dimensional dilution factor that quantifies the ratio of the entrained volume flux to the source volume flux. In Appendix A, we place these parameters in the context of previous work, and demonstrate how they may be related to the characteristic length scales of the flow.

P and θ can be thought of as ratios of time scales, pointing to the qualitative difference between our results and those of BT69 and WH83. Previous studies have used as a characteristic time scale the entrainment, or filling-box time t_{fb}, which, for a plume with specific buoyancy flux F_0 in a room of height H and cross-sectional area A is given by

$$t_{fb} = \frac{5AH}{6\epsilon\pi} \left(\frac{10}{9\epsilon F_0 H^5} \right)^{1/3}. \tag{2.5}$$

(BT69 and WH83 used the related time scale $(9/10)^{4/3} t_{fb}/3$.) The time scale given by (2.5) is the ratio of the volume of the room to the volume flux of a buoyant plume of source buoyancy flux F_0 as a result of entrainment during ascent through the room. It represents the time required to entrain and mix the fluid in the room through the plume, if the plume properties are determined exclusively by the source specific buoyancy flux.

However, if the source has non-zero volume flux, there are two other characteristic time scales for the flow within the room. Just as the filling-box time is associated with the source buoyancy flux, these two time scales are associated with the source (specific) momentum flux M_s and source volume flux Q_s. First, a time scale t_m can be defined using the source momentum flux, M_s, and it takes the form

$$t_m = \frac{AH}{2\pi\epsilon M_s^{1/2} H}. \tag{2.6}$$

This time scale, which we shall refer to as the momentum entrainment time scale, represents the time required for a turbulent jet, with momentum flux M_s, to entrain and mix the fluid in the room. This is analogous to the filling-box time scale. If the source also has non-zero volume flux, Q_s, there is a further characteristic time scale, the fluid replacement or turnover time

$$t_v = AH/(\pi Q_s). \tag{2.7}$$

The time t_v represents the time required to replace all the fluid in the room with input fluid, in the complete absence of mixing. In this paper, we are interested in the long time mixing and density evolution of the room, and so we have adopted this latter time scale as the characteristic time scale.

The parameters θ and P can be expressed as

$$\theta \equiv \frac{t_v}{t_m}, \quad P \equiv \left(\frac{5}{3} \right)^5 \frac{t_m^4}{t_v t_{fb}^3}, \tag{2.8}$$

with F_s replacing F_0 in (2.5). Our asymptotic results apply for $P \ll 1$, i.e. $t_{fb}^3 \gg t_m^4/t_v$, and in this limit, the ratio of the time scales t_v and t_m, as given by θ, determines the evolution of the concentration distribution within the room. In § 4, we highlight the qualitatively different behaviour of our predictions from that considered by BT69 and WH83 in the light of these time scales.

The plume concentration C_p, the ambient concentration C_a, and the vented concentration C_v are defined as

$$C_p(\zeta,t) = \frac{\rho_{a0} - \overline{\rho_p}(\zeta,t)}{\rho_{a0} - \rho_s}, \quad C_a = \frac{\rho_{a0} - \rho_a}{\rho_{a0} - \rho_s}, \quad C_v = \frac{\rho_{a0} - \rho_v}{\rho_{a0} - \rho_s}. \tag{2.9}$$

These concentrations range between zero (initial ambient fluid) and one (source fluid).

Assuming Q satisfies (2.3), C_p and C_a can be related by

$$C_p(\zeta,t) = \frac{1 + \theta \int_0^\zeta C_a(u,t)\,\mathrm{d}u}{1 + \theta\zeta}. \tag{2.10}$$

From (1.8), C_a evolves according to the non-dimensional advection equation

$$\frac{\partial C_a}{\partial \tau} = (1 + \theta\zeta)\frac{\partial C_a}{\partial \zeta}, \quad \tau = \frac{\pi Q_s t}{AH} = \frac{t}{t_v}\,. \tag{2.11}$$

Henceforth, we consider non-dimensional variables C_p, C_a, ζ and τ.

In the enclosed space, the concentration of the plume at the ceiling of the room, $C_p(1,\tau)$, equals the ambient concentration, $C_a(1,\tau)$, at the ceiling of the room. Assuming that there is a single ventilation opening at the same elevation as the plume source, and using (2.11), C_a is constant along characteristics η defined by

$$\frac{1}{\theta}\log(1 + \theta\eta) = \tau + \frac{1}{\theta}\log\left[1 + \theta\zeta\right]. \tag{2.12}$$

Therefore, the time τ at which a particular concentration surface is at a given depth ζ can be related to the (previous) time τ_ζ when that concentration surface is at the top of the room, $\zeta = 1$:

$$\tau_\zeta = \tau - \frac{1}{\theta}\log\left(\frac{1+\theta}{1+\theta\zeta}\right). \tag{2.13}$$

The (non-dimensional) residence time τ_r for concentration surfaces to migrate from the roof ($\zeta = 1$) to the vent ($\zeta = 0$) is given by

$$\tau_r = \tau - \tau_0 = \frac{1}{\theta}\log(1+\theta), \tag{2.14}$$

where τ_0 is τ_ζ as defined in (2.13), with $\zeta = 0$, the source height, i.e. the (non-dimensional) time that the concentration surface at the source was at the top of the room, $\zeta = 1$.

Under the assumption that $P \ll 1$, as defined in (2.2), the first fluid from the plume that arrived at the ceiling at time $\tau = 0$ (the so-called first front) reaches the source height $\zeta = 0$ at time $\tau = \tau_r$, and leaves through the vent. Therefore,

$$C_a(\zeta,\tau) = \frac{1 + \theta \int_0^1 C_a(u,\tau_\zeta)\,\mathrm{d}u}{1+\theta}, \tag{2.15}$$

and in particular

$$C_a(0,\tau) = \frac{1+\theta\int_0^1 C_a(u,[\tau-\tau_r])\,\mathrm{d}u}{1+\theta} = \frac{1+\theta\overline{C_a}(\tau-\tau_r)}{1+\theta}, \tag{2.16}$$

defining the mean ambient concentration within the room $\overline{C_a}$. Global conservation of $\overline{C_a}$ implies

$$\frac{\mathrm{d}\overline{C_a}}{\mathrm{d}\tau} = 1 - C_v(\tau) = 1 - C_a(0,\tau), \quad \overline{C_a}(0) = 0, \tag{2.17}$$

since the ambient fluid is initially completely uncontaminated by source fluid.

For times $\tau < \tau_r$, the first front has not yet reached the source, and so

$$\overline{C_a}(\tau) = \tau. \tag{2.18}$$

Once the first front has reached the vent, substituting (2.16) into (2.17) yields

$$\frac{\mathrm{d}\overline{C_a}}{\mathrm{d}\tau} = \frac{\theta}{1+\theta}\left[1-\overline{C_a}(\tau-\tau_r)\right]\ . \tag{2.19}$$

Once $\overline{C_a}(\tau)$ is known for the time interval $(n-1)\tau_r < \tau < n\tau_r$ ($n > 0$ an integer) we may find $\overline{C_a}(\tau)$ during the interval $n\tau_r < \tau < (n+1)\tau_r$ by integration of (2.19). Therefore, for the interval $n\tau_r < \tau < (n+1)\tau_r$, for $n \geqslant 1$ the concentration is given by

$$\overline{C_a}(\tau) = \lambda_n + (-1)^n\left(\frac{\theta}{1+\theta}\right)^n \frac{\tau_n^{n+1}}{(n+1)!} + \sum_{k=1}^{n}(-1)^{k+1}\left(1-\lambda_{(n-k)}\right)\left(\frac{\theta}{1+\theta}\right)^k \frac{\tau_n^k}{k!}, \tag{2.20}$$

$$\tau_n = \tau - n\tau_r, \quad \lambda_0 = 0, \quad \lambda_1 = \tau_r, \tag{2.21}$$

$$\lambda_n = \lambda_{n-1} + (-1)^{n-1}\left(\frac{\theta}{1+\theta}\right)^{n-1}\frac{\tau_r^n}{n!} + \sum_{k=2}^{n}(-1)^k\left(1-\lambda_{(n-k)}\right)\left(\frac{\theta}{1+\theta}\right)^{k-1}\frac{\tau_r^{k-1}}{(k-1)!}, \quad n \geqslant 2. \tag{2.22}$$

Although (2.22) provides an exact solution for the problem, it is somewhat unwieldy, and an accurate, approximate solution may be derived by noting that equation (2.19) admits exponential solutions of the form

$$1 - \overline{C_a} = a_1\exp(-\theta(\tau-\tau_r)) + a_2\exp(-\theta\phi(\tau-\tau_r)), \tag{2.23}$$

where ϕ is the root of the indicial equation

$$\phi = (1+\theta)^{(\phi-1)}. \tag{2.24}$$

Although these solutions do not satisfy the boundary conditions exactly, a good approximation may be derived by choosing the constants a_1 and a_2 such that this solution exactly matches the power series solution at the time $\tau = \tau_r$, when the plume fluid first exits from the vent,

$$\overline{C_a}(\tau_r) = \tau_r, \quad \left.\frac{\mathrm{d}\overline{C_a}}{\mathrm{d}\tau}\right|_{\tau=\tau_r} = 1 - C_f = \frac{\theta}{1+\theta}, \tag{2.25}$$

where C_f is the concentration of the first front, the leading contaminated fluid that has come from the plume rising through a completely uncontaminated room. As is

shown in § 3, this approximate solution is in very good accord with the full solution, even during the early times, $\tau = O(\tau_r)$.

The approximate asymptotic solution (2.23) predicts that the deviation $1 - \overline{C_a}$ of the mean concentration from pure source fluid consists of two decaying parts, with non-dimensional time scales $\tau_1 = 1/\theta$ and $\tau_2 = 1/(\phi\theta)$. The time scale $\tau_1 = t_m/t_v$ corresponds to the non-dimensional entrainment or filling-box time scale for a momentum-dominated plume. The approximate analytical solution proves very instructive particularly in the two extremes of $\theta \gg 1$ and $\theta \ll 1$.

In the limit of substantial dilution in the plume, $\theta \gg 1$, $\phi \to 1/\theta \ll 1$, and so $\tau_2 \sim 1$, which corresponds to the fluid replacement time. However, in this case, the time scale for mixing $\tau_1 \ll 1$ is very fast, corresponding to a plume which mixes the room rapidly through entrainment. We deduce that the adjustment is two-fold: initially there is a rapid adjustment over the time $\tau_1 \sim 1/\theta$, at the end of which $\overline{C_a} \ll 1$; then, over the time scale $\tau_2 \sim 1$, $\overline{C_a} \to 1$ exponentially.

Indeed, the limit $\theta \to \infty$ corresponds to the case of a well-mixed room with no vertical variation in concentration. The flow of pure source fluid (with concentration $C_p = 1$) into the room must then be balanced by an equal flow of ambient well-mixed fluid with concentration $\overline{C_a}$, so that

$$\frac{\mathrm{d}\overline{C_a}}{\mathrm{d}\tau} = 1 - \overline{C_a}, \quad \overline{C_a} \sim 1 - \mathrm{e}^{-\tau} \tag{2.26}$$

using the appropriate boundary condition that $\overline{C_a} = 0$ when $\tau = 0$.

In the opposite limit in which there is little dilution in the plume, $\theta \ll 1$, $\phi \gg 1$. For this limit, the arrival time of the first front $\tau_r \sim 1$ and corresponds to the fluid replacement time. Indeed, in this limit the volume flux of the plume varies little by entrainment, and the speed of descent of concentration surfaces (given by (1.7) and (2.3)) is essentially constant. Entrainment and mixing by the plume is so slow that the stratification in the room essentially consists of a step-like profile, with a layer of unmixed fluid (with $C_a \sim 1$) propagating down towards the source at a close to constant speed. When the front arrives, $\overline{C_a} \sim 1$.

Care needs to be taken in the interpretation of flows in this limit due to the large volume flux of fluid into the room from the source. As discussed in BT69, the depth of the outflowing layers that develop when the plume arrives at the ceiling should be of the order of the plume radius at the ceiling. As discussed in more detail in Appendix A, in this limit the effective source radius $b_s > H$, and so although very little entrainment occurs in the limit of small θ, it is to be expected that the outflowing layer will have a significant depth compared to H. However, such a layer of fluid can only appear on a time scale of the order of the replacement time scale (i.e. $\tau \sim 1$) as this is the time scale over which such a volume of fluid enters the room from the source. Indeed, to leading order this layer increases in depth linearly with time as the source fluid enters the room, and undergoes very little entrainment as it spreads and fills the room. Therefore, for small θ the adjustment of the mean concentration to that of pure source fluid occurs essentially linearly with time, whereas for a vigorous plume with $\theta \gg 1$ the mixing is exponential with time.

The solutions for the mean ambient concentration ((2.18) and (2.20)) may be used to determine the concentration at any height in space by combining equations (2.13), (2.15), and (2.16) to give the expression

$$C_a(\zeta, \tau) = \frac{1}{1+\theta} + \frac{\theta \overline{C_a}(\tau_\zeta)}{1+\theta}. \tag{2.27}$$

The variation of the concentration with time can be shown to be dependent on height in general, in contrast to the asymptotic assumption of BT69 and WH83, a consequence of $C_a \to 1$ as $\tau \to \infty$ everywhere within the room. In the next section, we explore the behaviour of the full model for larger values of the quantity P, defined in (2.2).

3. Numerical solutions

To solve the full problem defined by equations (1.4)–(1.6), (1.7) and (1.8) with given constant source conditions Q_s, M_s and ρ_s we have adopted the numerical integration scheme of Germeles (1975). The scheme relies on a discretization of the ambient density field (or equivalently the concentration field) into a finite number of 'layers' separated by sharp 'interfaces' or 'levels'. The evolution of the plume through the height of the room is assumed to occur much more rapidly than the evolution of the ambient density field within the room. The plume equations (1.4)–(1.6) are first solved using the (static) discretized layerwise density field, which is then advected towards the source by using a discretization of (1.8) with the appropriate velocity being determined using (1.7). Volume is conserved by introducing a new layer at the ceiling of the room, with volume given by the volume flux through the uppermost interface multiplied by the time step. The concentration is determined by noting that the fluid must come from the rising plume (see Germeles 1975 for a more detailed discussion).

In figure 2, we consider the time variation of the mean ambient concentration $\overline{C_a}$ in flows with nine different initial conditions, corresponding to three different values of θ, (0.1, 1 and 10) and three different values of the parameter P_0 (0.1, 1 and 10) as defined in (2.2). For all the cases shown here, there is excellent agreement between the theoretical prediction of the exact asymptotic model and the full numerical results.

In contrast to the well-mixed model, the exact asymptotic model also predicts the vertical distribution of the ambient concentration $C_a(\zeta, \tau)$, by use of (2.13), (2.15) and (2.16). For the same nine simulations as are shown in figure 2, in figure 3, we compare the vertical profiles of ambient concentration determined by the full model (plotted with a solid line) and the aysmptotic model (the solution to (2.20) and plotted with a dashed line) for twenty times $\tau = n/4$ for $n = 1 \ldots 20$. In general the agreement is good, particularly at later times as $P(t)$ inevitably drops to small values.

Since $C_v < \overline{C}_a$, the well-mixed model always over-estimates the concentration of the fluid leaving the room and hence under-estimates $\overline{C}_a$. For the flows with smaller θ, it is clear from figure 3 that the first front arrives at the vent substantially later than for the flows with larger θ. This later arrival is the cause of the sharp change of the rate of increase of $\overline{C}_a$ in figure 2(*a–c*), and is well-predicted by the reduced models. Before the first front arrival, $\overline{C}_a$ linearly increases (see (2.18)). After the first front reaches the vent, the rate of change of $\overline{C}_a$ decreases markedly, since contaminated fluid is being vented from the room. This sharp change in behaviour is not apparent for flows with larger θ, since for these flows the arrival time of the first front at the vent occurs on the filling-box or entrainment time scales, i.e. $\tau_r \sim \tau_1 \sim 1/\theta \ll 1$. The weak concentration gradients for flows with large values of θ, and thus significant amounts of plume entrainment, are the result of thorough mixing by the plume over the time of interest, and so the difference between the well-mixed model and the exact solution is small.

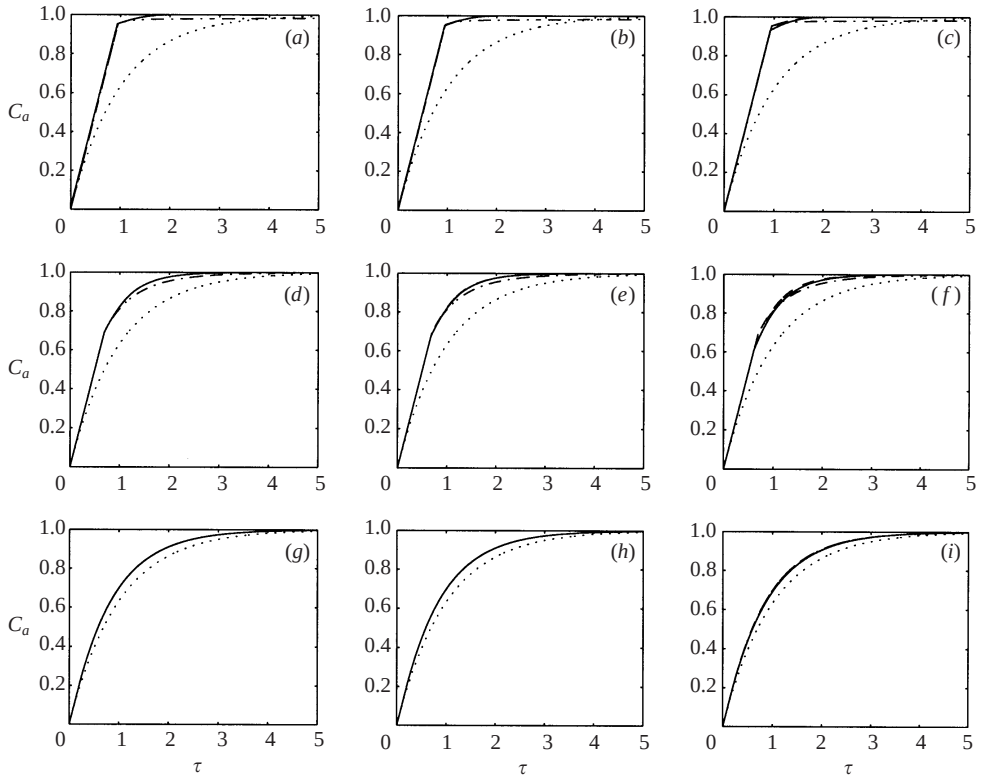

FIGURE 2. Comparison of the variation with time of the mean concentration $\overline{C}_a$ for the full solution of the numerical system (shown with a solid line), the full asymptotic solution (given by (2.20) and shown with a dashed line), the approximate exponential solution (defined by (2.23) and plotted with a dot-dashed line), and the well-mixed model ((2.26) and plotted with a dotted line) for flows with (*a*) $\theta = 0.1$, $P_0 = 0.1$; (*b*) $\theta = 0.1$, $P_0 = 1$; (*c*) $\theta = 0.1$, $P_0 = 10$; (*d*) $\theta = 1$, $P_0 = 0.1$; (*e*) $\theta = 1$, $P_0 = 1$; (*f*) $\theta = 1$, $P_0 = 10$; (*g*) $\theta = 10$, $P_0 = 0.1$; (*h*) $\theta = 10$, $P_0 = 1$; (*i*) $\theta = 10$, $P_0 = 10$; as defined in (2.4) and (2.2).

4. Comparison with the experiments of BT69

In the previous section, we showed that once all the fluid within the room has been cycled through a finite volume flux plume, the density distribution evolves towards the density of the input fluid. It is interesting to compare our analysis with the earlier works BT69 and WH83, as the asymptotic approach $C_a \to 1$ at all heights is qualitatively different from the predictions of the classical filling-box flow, associated with a pure source of buoyancy (as discussed in BT69). In that case, as mentioned in the Introduction, since there is no flow from the source, the plume density at the source is singular and so for a positive source of buoyancy, the models predict that the density in the room decreases without limit (WH83). In BT69 and WH83, only the simple situation in which $Q_s = M_s = 0$ was considered. As a result, $t_m \to \infty$ and $t_v \to \infty$ (as defined in (2.6) and (2.7)) and the parameters θ and P_0 are determined by considering the limits for these parameters as both $Q_s \to 0$ and $M_s \to 0$. It is well known (see e.g. Turner 1979, 1986) that for a plume rising from a point source of buoyancy flux, F_0, with $Q = M = 0$ at the source, into an unstratified ambient, there is a similarity solution given by

$$Q(z) = \frac{6\epsilon}{5}\left(\frac{9\epsilon}{10}\right)^{1/3} F_0^{1/3} z^{5/3}, \quad M(z) = \left(\frac{9\epsilon}{10}\right)^{2/3} F_0^{2/3} z^{4/3}, \tag{4.1}$$

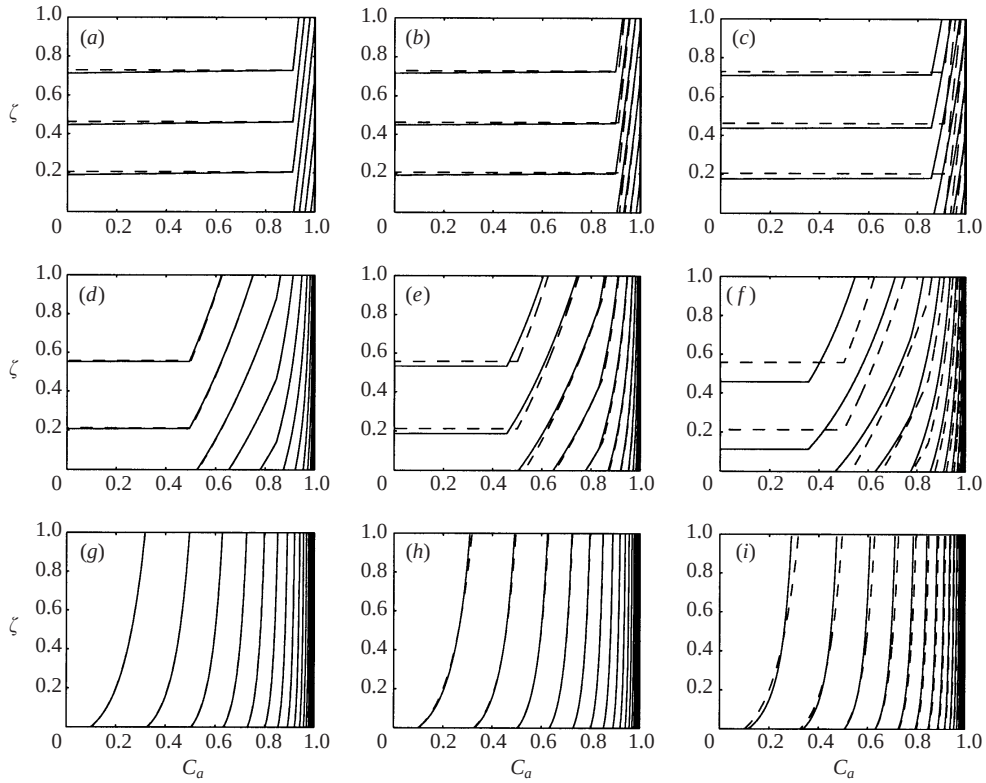

FIGURE 3. Comparison of the variation with time of ambient concentration profiles $C_a(\zeta, \tau)$ for the full solution of the numerical system (shown with a solid line) and the full asymptotic solution (given by (2.20) and shown with a dashed line) at times $\tau = n\tau_r/4$ where $n = 1 \ldots 20$ and τ_r is as defined in (2.14) for flows with (*a*) $\theta = 0.1$, $P_0 = 0.1$; (*b*) $\theta = 0.1$, $P_0 = 1$; (*c*) $\theta = 0.1$, $P_0 = 10$; (*d*) $\theta = 1$, $P_0 = 0.1$; (*e*) $\theta = 1$, $P_0 = 1$; (*f*) $\theta = 1$, $P_0 = 10$; (*g*) $\theta = 10$, $P_0 = 0.1$; (*h*) $\theta = 10$, $P_0 = 1$; (*i*) $\theta = 10$, $P_0 = 10$; as defined in (2.4) and (2.2).

and so the appropriate forms of θ and P_0 are

$$P_{pb} = \theta_{pb} = \lim_{z \to 0} \frac{5H}{z} \to \infty. \tag{4.2}$$

Therefore, the models BT69 and WH83 only apply for the initial stages of mixing when the source momentum flux is small and our momentum-driven asymptotic model is not applicable owing to the large value of the parameter P_0.

By assuming that the plume buoyancy flux is uniformly distributed throughout the room through entrainment, BT69 were able to estimate the ambient density profile. They showed that, subject to this assumption, the non-dimensional asymptotic profile, labelled f_0 in BT69, is given by the expression

$$f_0 = -\left(\frac{10}{9}\right)\left(\frac{15}{2}\right)^{1/3} \frac{t}{t_{fb}} + \left(\frac{5AH}{3\pi F_0 t_{fb}}\right)\left(\frac{5}{9}\right)^{1/3} \frac{g(\rho_a - \rho_0)}{\rho_0} \tag{4.3}$$

$$\simeq 5\left(\frac{5}{18}\right)^{1/3}\left[\zeta^{-2/3}\left(1 - \frac{10}{39}\zeta - \frac{155}{8112}\zeta^2\right) - \frac{1959}{2704}\right], \tag{4.4}$$

where the buoyancy flux has been set to be zero at the ceiling $\zeta = 1$.

However, real experiments such as those presented by BT69 do involve small, yet finite values of the source volume and momentum fluxes and hence finite values for

the time scales t_v and t_m and the parameters θ and P_0. The models proposed by BT69 and WH83 are therefore only strictly valid during times short compared to the fluid replacement time for flows in which $t_{fb} \ll t_v$. This restriction may be expressed in terms of the dimensional source parameters as

$$\left(\frac{3}{4}\right)\left(\frac{6\epsilon}{5}\right)^4 g_0' H^5 \gg Q_s^2, \tag{4.5}$$

where g_0' is the initial source reduced gravity as defined in (2.1).

In their experiments, plume flow within an enclosed space was modelled by a source of dense salty fluid at the top of a tank, descending through fresh water. The depth of water in the tank was allowed to increase, under the assumption that the hydrostatic pressure change associated with this increasing depth had little dynamic effect on the flow evolution. This experimental situation corresponds to a source at the same height as the vent within our formalism. The initial density difference between the salty plume fluid and the fresh room fluid was 13%–16%. The cross-sectional area of the tank was $2.5 \times 10^3\,\mathrm{cm}^2$, and the effective depth of the room was varied between 17.5 cm and 36 cm. Also, the source buoyancy flux was varied in the range 66–$128\,\mathrm{cm}^4\,\mathrm{s}^{-3}$ by variation of the density difference between the source and ambient and through variation of the source volume flux. These data imply that for the experiments reported, the filling-box time scale varies in the range $t_{fb} \simeq 300$–$500\,\mathrm{s}$, while the fluid replacement time scale is significantly longer, $t_v \simeq 6 \times 10^4$–$2 \times 10^5\,\mathrm{s}$. We therefore expect that, for times equal to or in excess of the filling-box time, then the mass flux will have an important effect on the evolution of these experiments.

In order to compare our model with their results, we have estimated an appropriate value of θ for the data presented by BT69 in two ways, as discussed in Appendix B, and to a reasonable approximation, it appears that θ took three characteristic values, 45, 65 and 85 in the experiments. We show the 'dimensionless density defect', a rescaled version of (4.4) given by

$$\frac{g[\rho_a(\zeta) - \rho_a(1)]H^{5/3}}{\rho_0(\pi F_0)^{2/3}} = \frac{f_0}{(4\pi\alpha^2)^{2/3}} = [C_a(\zeta) - C_a(1)]\left(\frac{F_0 H^5}{\pi^2 Q_s^3}\right)^{1/3}, \tag{4.6}$$

from these experiments in figures 4(a), 4(b) and 4(c) respectively. In this expression α is the experimentally determined entrainment constant under the assumption of Gaussian profiles of density and velocity within the plume, which was found to be equal to 0.1, by consideration of the propagation speed of the first front (see Appendix B). As is well-known, (see e.g. Turner 1979, 1986) the top-hat entrainment coefficient ϵ used throughout this paper is linearly related to the Gaussian entrainment constant α associated with the experimentally observed profiles, such that $\epsilon = \sqrt{2}\alpha$.

It is apparent that the experimental density profile has larger values than the approximate model prediction of BT69, especially in the vicinity of the source. For comparison, we also present the numerical predictions of our model (i.e. (2.27) rescaled as on the right-hand side of (4.6)) using source conditions given by the appropriate value of θ, and assuming $P_0 = \theta$, at the non-dimensional times $\tau_e = t_e/t_v$, where t_e is the reported time of the experimental measurement. Allowing for the small, yet finite source volume flux provides a more accurate description of the experimentally observed density profiles, particularly in the vicinity of the source. The very good comparison of our model predictions with the data supports the simplifying assumption we have made that $P_0 = \theta$ as is discussed in more detail in Appendix B.

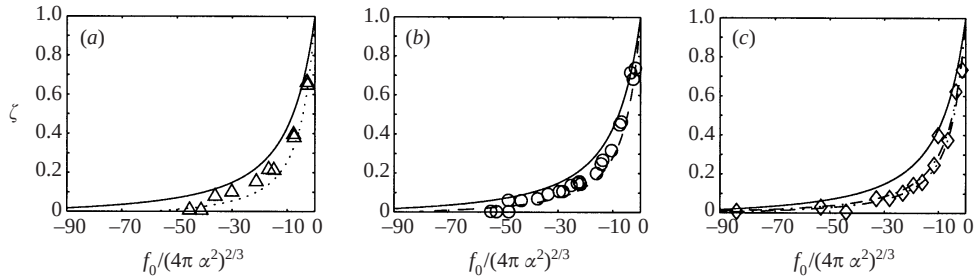

FIGURE 4. Comparison of the theoretical prediction for the dimensionless density deficit profile with height ζ due to BT69 and defined in (4.6) (shown with a solid line), the experimental measurements reported in BT69 for various flow conditions (shown with symbols), and the numerical profiles from calculations with the same estimated source conditions, measurement time and scaling (shown with broken lines): (*a*) $\theta \simeq 45$, $P_0 \simeq 45$, $17.5\,\mathrm{cm} < H < 19\,\mathrm{cm}$, $\tau_2 = 0.22$; (*b*) $\theta \simeq 65$, $P_0 \simeq 65$, $27.5\,\mathrm{cm} < H < 32.5\,\mathrm{cm}$, $\tau_2 = 0.14$; (*c*) $\theta \simeq 85$, $P_0 \simeq 85$, $H < 36\,\mathrm{cm}$, $\tau_2 = 0.09$, $\tau_3 = 0.28$.

We conclude by reiterating that the assumption of BT69 that the ambient density changes linearly with time can only apply for times early compared to the fluid replacement time t_v, even for such flows with large dilution parameters θ. This is because the stratification becomes eroded by the continual outflow of fluid from the room. We deduce that any finite volume flux at the source causes the density profile to evolve away from the approximate density profile defined in BT69 for times in excess of t_v.

5. Application example

In real applications, it may be the case that the dilution factor θ is substantially smaller than in the laboratory. Therefore, the behaviour of real systems may well be qualitatively different from the experimentally investigated flows with high entrainment, and yet be described well by the finite-source volume flux model developed in § 2. One important class of application is the case of a cold air supply from a ceiling-mounted (and vented) air-conditioner, to a room of cross-sectional area of the order of $A = 100\,\mathrm{m}^2$ and height $H = 4\,\mathrm{m}$, such as a meeting or lecture room. If we assume that the initial temperature difference between the air-conditioned air and the air inside the room is of the order of 10 °C, then $g_0' \sim 0.3\,\mathrm{m\,s^{-2}}$. If the room has about fifty occupants, then in order to maintain comfortable air quality, a ventilation flow of order $1\,\mathrm{m^3\,s^{-1}}$, would be required. For a ventilation opening of area $1\,\mathrm{m}^2$ which allowed inflow of cold air from the air-conditioning unit at the top of the room, there would be a high-Reynolds-number turbulent flow at the source with $w_s \sim 1\,\mathrm{m\,s^{-1}}$.

In this case, the filling-box time would be $t_{fb} \simeq 500\,\mathrm{s}$, while the fluid replacement time is $t_v \simeq 400\,\mathrm{s}$, and so $\theta \simeq P_0 \simeq 1.4$. Since the filling-box time is comparable to the fluid replacement time, we expect the ambient stratification to retain considerable vertical structure until the first front vents from the room. The system will then converge to a uniform steady state. For this example we assume that the vent from the space is close to the same height as the source (i.e. near the ceiling). In figure 5(*a*) we show the evolution of the mean temperature within the room towards that of the air-conditioned air (solid line) and compare it both to the prediction of our asymptotic model (dashed line) (given by (2.18) and (2.20)) and the well-mixed model (dotted line) (2.26). For a significant period of time (of the order of 10–15 minutes) the mean temperature in the room is over-estimated by 2–3 °C by the well-mixed

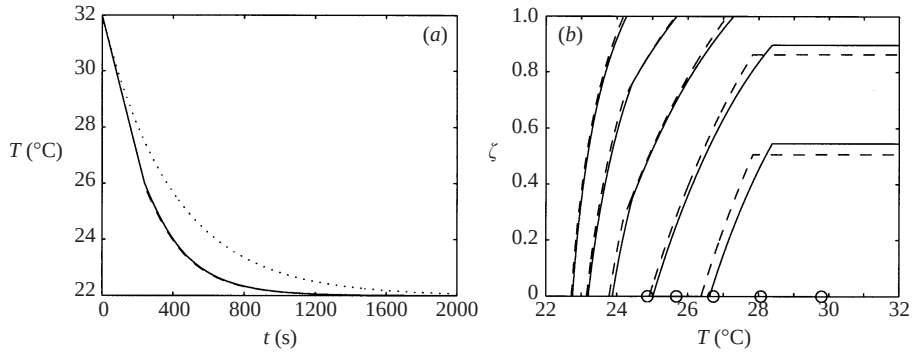

FIGURE 5. (*a*) Comparison of predictions of the mean temperature within a room, initially at 32 °C, which is cooled with conditioned air at 22 °C given by the full solution of the numerical system (shown with a solid line), the full asymptotic solution (given by (2.20) and shown with a dashed line), the well-mixed model ((2.26) plotted with a dotted line) for a flow with $\theta = 1.4 = P_0$, and $t_v = 400$ s as defined in (2.4), (2.2), and (2.7). (*b*) Comparison of the variation with time of ambient temperature profiles for the full solution of the numerical system (shown with a solid line), and the full asymptotic solution (given by (2.20) and shown with a dashed line) at times $t = 100n$ s where $n = 1 \ldots 5$ for our application example. The circles denote the predicted temperature from the well-mixed model (2.26) at these five times. Time increases from right to left.

model, while our asymptotic model agrees extremely well with the full numerical model. The origin of these differences may be understood by examining the evolution of the temperature profile.

In figure 5(*b*) we show the temperature profile at five times during the flow development, and compare these profiles with the predictions of the well-mixed model (2.26) shown as circles on the x-axis of the figure. Note, for clarification, that in this example, the vent and source are both at the ceiling ($\zeta = 1$) and the temperature decreases with time due to the air conditioning, and so these profiles are inverted compared to those shown in figure 3. Our asymptotic model (dashed line) predicts the vertical temperature distribution in the room (solid line) very accurately. The well-mixed model (circles) under-estimates the temperature at early times at the vent ($\zeta = 1$) since it does not capture the vertical stratification within the room. In particular, the calculations identify that a hot layer of fluid persists near the ceiling for some time. Therefore, in contrast to our approximate analytical model, the very simple well-mixed model under-estimates the amount of heat leaving the room due to the displacement of room air by the inflow from the air conditioner, and over-estimates the temperature within the room, in particular at low levels, for a few fluid replacement times (approximately 30 minutes).

Although the model has been applied to interpret the transient evolution of the density resulting from a source of cooling fluid supplied to a room, the model can also be used to interpret the transient dispersion of smoke or poisonous gases which may leak into an enclosed space. For example, the model presented in § 2 could be used to identify optimal locations for sensors of noxious gases or smoke, so as to maximize the time available to occupants for evasive action.

6. Conclusions

In this paper, we have considered the flow within an enclosed space with a single vent and a localized continuous source of fluid of different density, which we

have modelled as a buoyant plume. We have found that once all the fluid initially within the room has been cycled through the plume by turbulent entrainment the density of the fluid within the room tends towards the density of the source fluid. If the source volume flux is small compared to the volume flux entrained during the motion of the plume across the vertical extent of the room, then we predict that the room becomes close to well-mixed, with the ambient density approaching the density of the source fluid exponentially with time. For very early times this exponential convergence appears to correspond to a linear variation with time, as postulated in previous laboratory work (BT69). Nevertheless, inclusion of the finite-source volume flux in our model quantitatively improves the description of these flows. Conversely, if the plume entrains very little fluid as it rises through the room, we find that in the long-time limit the room density converges approximately linearly to that of the source fluid. As well as a full numerical solution of the equations describing the evolution of the plume and ambient fluid, we have developed approximate analytical models that can describe accurately both the temporal and spatial variation of the concentration in the room. These models are based on the realization that with a finite-source mass flux, in the long-time limit the momentum flux of the plume inevitably varies little as the plume rises within the room.

There are numerous additional challenges in this area for applying the theory of turbulent plumes and classical filling-box theory to flows involving a net mass flux as well as more complex room geometry. We are at present examining the flows which arise in a room with one or more ventilation openings at different heights from the source in addition to an imposed mass flux and will report on those issues in subsequent contributions.

Appendix A. Relationships involving θ and P_0

Here we examine the connection between our parameters P and θ and parameters which have been introduced in previous work. First, we note that the ratio P/θ corresponds exactly to the momentum flux parameter Γ discussed by Morton (1959) which classifies sources in an unbounded ambient:

$$\Gamma = \frac{P}{\theta} = \frac{5F_sQ_s^2}{8\epsilon M_s^{5/2}}. \tag{A 1}$$

$\Gamma = 1$ corresponds to so-called 'pure plume balance', i.e. the plume appears to be rising from a source of buoyancy alone at some distance below the actual source, while $\Gamma < 1$ describes forced plumes, with an excess of source momentum flux, and $\Gamma > 1$ describes distributed or 'lazy' plumes, with a deficiency of source momentum flux, or equivalently, a source too large for pure plume balance for the given value of Q_s (Caulfield & Woods 1995; Hunt & Kaye 2001). Γ also corresponds to the inverse square of a Froude number, comparing the relative importance of the buoyancy to the source velocity.

The parameters defined here can also be interpreted as ratios of length scales. From (1.4)–(1.6), we write

$$Q_s \equiv w_s b_s, \quad M_s \equiv w_s^2 b_s^2, \quad F_s \equiv g_s' w_s b_s^2, \tag{A 2}$$

defining an effective source radius and velocity. Therefore, it is apparent that θ is essentially the inverse of the non-dimensional effective source radius, i.e. $\theta = 2\epsilon H/b_s$. Large values of θ can thus be thought of as corresponding to small sources (thus

subject to significant increases in volume flux through entrainment as the plume rises in the room) while smaller values of θ correspond to larger sources, with significantly less entrainment as the plume rises. Since the volume conservation relation (1.7) requires that the plume occupies a negligible fraction of the cross-sectional area A of the room, a further implicit assumption of our model is that $b_s \ll A$.

Similarly, the parameter P can be related to a ratio of length scales. The characteristic length scale over which the source momentum flux is important compared to the source buoyancy flux is the jet length L_j (List 1982), while the characteristic length scale over which the source volume flux is important compared to the source buoyancy flux is the 'acceleration length' (see Caulfield & Woods 1995) L_a:

$$L_j = \frac{M_s^{3/4}}{F_s^{1/2}}, \quad L_a = \frac{Q_s^{3/5}}{F_s^{1/5}}, \quad P = \frac{5}{4}\left(\frac{L_a}{L_j}\right)^{5/3}\frac{H}{L_j}. \tag{A 3}$$

As F_s decreases, L_j and L_a increase, illustrating that the source buoyancy flux becomes less and less important.

Appendix B. Determination of experimental values of θ and P_0

To estimate the appropriate values of the parameters θ and P_0 for experimental flows, it is necessary to identify the specific momentum flux associated with the source. Near the source there may be a zone of flow establishment, especially if the Reynolds number of the flow at the source is sufficiently small (List 1982). For the experiments reported in BT69, the appropriate form for the Reynolds number is

$$Re = \frac{\pi F_0 R}{g_0' \pi R^2 \nu}, \tag{B 1}$$

where R is the source radius, and ν is the kinematic viscosity of water. Substituting the quoted values of g_0' and πF_0 into this expression, it appears that the exit Reynolds numbers were of the order of 50–100, and thus unlikely to be fully turbulent.

However, information about the actual relationship between M_s and Q_s in the laboratory can be inferred from consideration of the rate of descent of the first front of contaminated fluid towards the source. In the experimental configuration used in BT69, the speed of any density surface is given by (1.7). For the fluid ahead of the first front, since the plume is rising in an unstratified environment, so that the buoyancy flux of the plume is constant at its initial value F_0, it is possible to reduce (1.4)–(1.6) to the single equation

$$\frac{\mathrm{d}Q}{\mathrm{d}z} = \left(\frac{20\epsilon^4 F_0}{Q_s^3}\right)^{1/5}\left(\frac{Q}{Q_s} + \frac{[1-\Gamma]}{\Gamma}\right)^{1/5}, \tag{B 2}$$

where Γ is Morton's momentum flux parameter, as defined in (A 1). Irrespective of the value of Γ, solutions to (B 2) will ultimately tend towards a state of so-called 'pure plume balance' for which the plume appears to have risen from a source of pure buoyancy alone with an 'effective origin' z_e distinct from the actual origin.

If pure plume balance applies immediately upon leaving the source, $\Gamma = 1$, and then $Q(z)$ and $M(z)$ are given by (4.1) with $(z + z_e)$ replacing z on the right-hand sides of the equations, with $z = -z_e$ as the notional location of the effective origin. This can be combined with (1.7) to establish an implicit formula for the location of

the first front z_f with time:

$$t = \frac{5A}{4\pi}\left(\frac{10}{9\epsilon F_0(H+z_e)^2}\right)^{1/3}\left(\left[\frac{(H+z_e)}{(z_f+z_e)}\right]^{-2/3} - 1\right). \tag{B 3}$$

If this functional form for the relationship between the time t and the location of the first front z_f is found, then there is strong evidence that $\Gamma = 1$ (at least after any initial zone of flow establishment) and hence that pure plume balance pertains from near the source, as any other value of Γ inevitably leads to a different relationship between Q and z from (B 2), and hence a different relationship between t and z_f. As discussed in Appendix A, $\Gamma = 1$ further implies that $P_0 = \theta$.

BT69 showed for all their experiments that the analogue of (B 3) appropriate for (experimental) Gaussian profiles of velocity and density (i.e. replacing ϵ with $\sqrt{2}\alpha$, the Gaussian entrainment constant, as mentioned in § 4) did indeed describe well the time-dependence of the first front location for a particular value of the effective origin of the plume of the order of 0.8 cm. The comparison of the experimental data with the predictions of (B 3) also yielded the estimate of $\alpha \simeq 0.1$. The observation that the first front propagation speed is well-modelled by (B 3) suggests that to leading order it is appropriate to approximate the plume motion as being in pure plume balance for the turbulent plume flow in their experiments, although this may introduce some error in the vicinity of the source, where the solution of (B 2) may be different from the asymptotic form (B 3), which applies in the far field.

Therefore, the effective source conditions Q_s and M_s (and so $\theta = P_0$) can be expressed in terms of the effective origin z_e, the entrainment constant ϵ and the source buoyancy flux F_0 (all experimentally measured quantities):

$$Q_s = \frac{6\epsilon}{5}\left(\frac{9\epsilon F_0 z_e^5}{10}\right)^{1/3}, \quad M_s = \left(\frac{9\epsilon F_0 z_e^2}{10}\right)^{2/3}, \quad \theta = P_0 = \frac{5H}{3z_e}. \tag{B 4}$$

The observation of the propagation of the first front in a way that is consistent with pure plume balance allowed BT69 to measure directly the effective origin z_e, and this experimentally measured quantity can then be used to determine θ and P_0.

A second, independent method of determining z_e can be made indirectly using the expression for Q_s in (B 4) which can be reposed as an equation to determine the unknown z_e. For the experiments reported in BT69, these two distinct methods give values of z_e (and so θ and P_0) within 10% of each other, and so a reasonable first assumption is to suppose that $P_0 = \theta$. This is not a major constraint, as, particularly for such large values of θ, variations in P_0 are not all that significant in the evolution of C_a.

REFERENCES

Baines, W. D. & Turner, J. S. 1969 Turbulent buoyant convection from a source in a confined region. *J. Fluid Mech.* **37**, 51–80 (referred to herein as BT69).

Caulfield, C. P. & Woods, A. W. 1995 Plumes with non–monotonic mixing behaviour. *Geophys. Astrophys. Fluid Dyn.* **79**, 173–199.

Germeles, A. E. 1975 Forced plumes and mixing of liquids in tanks. *J. Fluid Mech.* **71**, 601–623.

Hunt, G. R., Cooper, P. & Linden, P. F. 2001 Thermal stratification produced by plumes and jets in enclosed spaces. *Building Environ.* **36**, 871–882.

Hunt, G. R. & Kaye, N. G. 2001 Virtual origin correction for lazy turbulent plumes. *J. Fluid Mech.* **435**, 377–396.

List, E. J. 1982 Turbulent jets and plumes. *Annu. Rev. Fluid Mech.* **14**, 189–212.

Morton, B. R. 1959 Forced plumes. *J. Fluid Mech.* **5**, 151–163.

Morton, B. R., Taylor, G. I. & Turner, J. S. 1956 Turbulent gravitational convection from maintained and instantaneous sources. *Proc. R. Soc. Lond.* A **234**, 1–23.

Turner, J. S. 1979 *Buoyancy Effects in Fluids*, 2nd Edn. Cambridge University Press.

Turner, J. S. 1986 Turbulent entrainment: the development of the entrainment assumption, and its application to geophysical flows. *J. Fluid Mech.* **173**, 431–471.

Worster, M. G. & Huppert, H. E. 1983 Time–dependent density profiles in a filling box. *J. Fluid Mech.* **132**, 457–466 (referred to herein as WH83).